TRACKING OF COHERENT THERMAL STRUCTURES ON A HEATED WALL. PART 2: DNS SIMULATION

T.A. KOWALEWSKI

Polish Academy of Sciences, IPPT PAN

Swietokrzyska 21, PL 00-049, Warszawa, Poland

Email: tkowale@ippt.gov.pl

Fax: +48-22-8269803

A. MOSYAK, G. HETSRONI

Department of Mechanical Engineering,

Technion – IIT, Haifa, 32000 Israel

Email: hetsroni@tx.technion.ac.il

Fax: +972-4-834-3362

Abstract

The aim of the paper is to correlate temporal evolution of a thermal pattern observed on a heated wall by infrared camera with the propagation velocity of the thermal perturbations calculated by DNS. In the experiment the propagation velocity was measured by using PIV-based analysis of infrared images of the thermal pattern on the wall. To verify the experimental technique of image analysis, a sequence of synthetic images, simulating thermal pattern on the wall was generated from the DNS solution and the convective velocity has been evaluated. It was found that the convective velocity of thermal structures obtained by PIV-based analysis of the experimental and synthetic images, is in relatively good agreement with that calculated from the DNS solution. For water the propagation velocity of the thermal perturbations is only about half of the convective velocity of the velocity perturbations. The present study confirms that the convection velocity observed for hot spots is distinctly lower than that for the cold spots.

1. Introduction

The turbulent flow structures are strongly influenced by interactions between the flow and the wall. Many studies have been devoted to the experimental investigation of this problem. Observed fluctuations of the flow indicate very distinct intermittency of the turbulent flow close to the boundary. It appears that particular quasi-periodic bursting structures can be identified in the wall layers. These events, of relatively short duration and pronounced turbulence activity, during which most of the turbulent energy is generated, consist of at least two phases: ejections of low momentum fluid masses from the near wall region, and injections of high-momentum fluid masses towards the wall. The ejections and the injections occur intermittently and in interaction with the flow, they produce high instantaneous fluctuations of the local heat or mass transfer at the wall. These fluctuations can be visualized by recording the instantaneous temperature fields at the wall (Kaftori et al. 1994, Hetsroni & Rozenblit 1994, Hetsroni et al. 1996, Irtani et al. 1983).

The correlation between the spatial characteristic of the thermal field and that of the velocity is an important issue of turbulence studies (Krogstad et al. 1998, Kawamura et al. 1998, 1999). If the temperature differences within the boundary layer are small, the buoyancy effects can be neglected. In such case, the thermal pattern convected by the flow may be considered as a passive scalar (Herman et al. 1998). Hence, non-intrusive measurements of instantaneous thermal fields within the flow and at the walls can deliver valuable information about turbulent characteristics of the flow. However, it is important to note that the passive scalar behavior can be strongly modified if local isotropy is violated. As it was pointed by Warhaft (2000), the existence of exponential tails in scalar signals while the velocity is Gaussian, the contrast between the scalar and velocity spectra and the anisotropy at dissipation and inertial scales, may play determining role for passive scalar characteristics, and additional findings seem to be necessary to find proper relations between momentum and heat transport for turbulent flow. Hence, understanding behavior of passive scalars appears to be a new challenging problem of great practical importance.

Much of the visual information concerning passive scalars has come from flow imaging of dye in liquids. However, these methods offer mainly bulk information. For near-wall studies, temperature as passive scalar appears to be an attractive alternative. One of the possible methods to visualize the presence of thermal structures is to use the thermography. It makes it possible to

acquire the information about the structures directly at the wall without introducing any flow perturbation. This is a very important issue, as the use of the most of the available flow analysis methods, like LDA, PIV or hot wire technique, is limited to large non-dimensional distances from the wall. A key question is whether the wall temperature measurements reflect scaling and response time of organized hydrodynamic structures.

In our previous paper (Hetsroni et al. 2001) it was shown that a relatively simple analysis of the thermal fluctuations observed on the wall, could be used to obtain turbulent characteristics of the underlying fluid flow. The proposed method may be attractive in many practical applications as it allows for the analysis of turbulence without any optical or mechanical access to the flow. It is well-known that in many problems of heat transfer the dominant mechanism is advective transport. In these situations it is particularly useful to adopt a Lagrangian viewpoint, with an observer following the motion of a collection of fluid particles that together constitute the fluid continuum. The description of turbulent transport in terms of convection velocity in fact dates back to the work of Taylor (1921). This point was investigated in the recent paper by Tiselj et al. (2001) with regard to the process of scalar transport. It was shown that convection velocities of scalar transport depends on Prandtl number and thermal wall boundary conditions. The main purpose of the present paper is to use data available from the numerical simulation of the flow to verify and refine the conclusions obtained on the convective velocity of the thermal structures and to confirm observed difference between convection velocity of “hot spots” and “cold spots”. It is shown that the thermal fluctuations observed on the wall in the experiment, actually correspond to the convective thermal structures identified within the bulk flow generated for the similar flow using the direct numerical simulation.

2. Formulation of the problem

We consider the experimental configuration described in the previous paper (Hetsroni et al. 2001). It consists of an open flume (4.3m long, 0.32m wide and 0.1m deep) with a pump forcing circulation of water with constant temperature. The flow depth is 0.037m and the hydraulic diameter is 0.066m. The water temperature at the inlet is $20^{o}C \pm 0.1^{o}C$. A fully developed turbulent flow is established in the region beyond 2.5m downstream from the inlet of the flume. At this distance a 170 x 135mm patch made of a 50μm thick constantan foil is mounted at the

bottom of the flume. The foil is heated by DC current to produce the constant heat flux $q = 12\ kWm^{-2}$. The temperature variations in the range of 2^oC are observed on the foil by an infrared radiometer. For small temperature variations the imposed buoyancy effects are negligible and temperature field behaves as a passive scalar. Hence, the temperature distribution on the wall can be considered as a trace of the flow structure near the bottom wall.

The measured value of average streamwise water velocity was U_o = 0.25m/s, the corresponding Reynolds number based on the water height is Re = 9200. The experimental value of shear velocity u^*=0.0133m/s agrees well with the *logarithmic law of the wall*: $U^+ = 2.5\ln(x_3^+) + 5.0$. Throughout this paper the streamwise direction is denoted by x_1, the spanwise direction by x_2, and the wall-normal direction by x_3, while the velocity components are u_1, u_2, u_3, correspondingly. U, V denote mean local flow velocity and perturbation velocity in the streamwise direction, respectively. Velocity, time and distance are normalized by wall units as $u_i^+ = u_i/u^*$, $t^+ = t\,u^{*2}/\nu$, $x_i^+ = x_i\,u^*/\nu$, where ν denotes the kinematic viscosity of fluid.

The above experimental configuration is investigated numerically using Direct Numerical Simulation (DNS) technique. However, it should be noted that due to the computational constrains the present DNS was performed at lower Reynolds number, i.e. at Re= 2600.

3. Experiment

The experiment is described in details elsewhere (Hetsroni et al. 2001), here we repeat only the main considerations. The experimental set-up consisted of an infrared scanner, S-VHS video recorder, computer, monitor and 8-bit frame grabber. The radiometer was located at a distance of 0.5m and the IR image created on the foil was recorded from below. The frequency response of heated foil used in the present experiments is 0.04s. It is short enough to investigate convection velocity of the thermal perturbations generated on the wall (Hetsroni et al. 2001).

The video frames were captured and digitized using the frame grabber and stored as 768x576 pixel images with the 256 levels of gray. Once a set of picture data had been digitally captured and stored, the result was a succession of 50 sequentially recorded image frames depicting the temperature field on the foil at discrete instances in time. The time interval between images, determined by the video rate, was equal Δt = 40ms, i.e. $\Delta t^+ = 7.04$. The image analysis used to determine convective velocity of a thermal pattern was based on the two-dimensional

correlation between thermal patterns found within the analyzed images. It was preformed applying the well-known Particle Image Velocimetry (PIV) approach to infrared images. The high resolution method (Quenot et al. 1998) used allowed us to evaluate convective velocity of the thermal spots at each pixel of the IR image.

A sequence of the temperature streaks observed at the wall starts with the rise of small moving temperature spots. These spots change their position and streamwise length (comp. Fig. 6 in Hetsroni et al. 2001). The high and low temperature streaks, clearly seen on the wall surface, indicate the presence of coherent structures advected by the main flow. The streamwise flow structures persist some time until a strong mixing (vertical burst) leads to their disappearance. These bursts are responsible for the local increase or decrease of the wall temperature, visible as the bright and dark patches on the IR image, and advected by the flow in the streamwise direction. We may note that the convection motion varies both in the direction as in the magnitude, but a strong streamwise velocity bias transporting thermal spots from left to right is clearly visible. Looking at a longer sequence of images it appears that the dark (cold) patches move faster and often overtake adjacent bright streaks. The high and low temperature streaks may interact with each other too.

The measured streamwise velocity fluctuations are related to the geometry of the streak pattern. The low and high-speed streaks passing the selected point of observation contribute to the transient pattern. For a sufficiently long observation time, their main characteristics become space independent. Then, analysis of the full field temporal behavior of both velocity components may deliver large amount of data for statistical analysis of the flow. But even our relatively short sequence may be used to evaluate the characteristic velocity of the observed thermal structures. For this purpose we need to identify them in the velocity vector field. We assume that they indicate the location of moving thermal spots. To evaluate their characteristic velocity, some discrimination technique must be applied.

In the present examination high temperature spots are selected discriminating the gray levels of the image in the arbitrary selected range from 175 to 255. The low temperature spots are detected choosing the gray level range from 0 to 100, selected so to get similar intensity histograms for both cases. It appears that the “hot” and “cold” structures have different velocity. Remembering that the wall temperature strongly depends on the third velocity component (from or to the wall), this difference in the convective velocity can be used to determine different coherent structures acting on the wall. Figure 1 shows velocity histograms obtained for the

sequence of 16 images evaluated separately for "hot and "cold" thermal spots. Looking at the velocity histogram (Fig. 1) we may note that the measured streamwise velocity characterizes very broad spectrum with a flat maximum close to $V_T^+ = 4$ for the hot spots and a slightly higher value for the cold spots. By taking the time and space average for the whole sequence, the mean velocity is obtained for hot spots equal to $V_T^+ = 3.76$ and for the cold spots $V_T^+ = 4.77$. Our hypothesis is that these values correspond to the mean propagation velocity of coherent flow structures responsible for the ejection bursts from the wall (positive temperature pulse) and for the injections of the fluid to the wall (negative temperature pulse – comp. Krogstad et al. 1998).

To verify this assumption it is necessary to correlate the results obtained from the analysis of thermal images with the corresponding flow structure within the channel. Experimentally such procedure is difficult to perform. The main reason is the difficulty in obtaining acceptable velocity and temperature measurements for small distances from the wall ($x_3^+ < 10$). Hence, we looked for the corresponding data obtained from direct numerical simulations (DNS) of the fully developed turbulent flow in an open channel.

4. DNS method and determination of convection velocity

The DNS solution obtained for a fully developed turbulent flow at Pr=0.71 and Pr=5.4 in open channel was used to analyze the convection velocity of thermal perturbations. Details of the numerical method and the turbulent data analysis are described by Tiselj et al. (2001) in a separate paper and here we only repeat its main points.

The time-dependent, three-dimensional Navier-Stokes and continuity equations were solved in a rectangular domain. The flow geometry and coordinate system are shown in Figure 2. The flow is driven by a constant streamwise pressure gradient. The boundary conditions are no-slip on the bottom wall, and free-slip on the free surface. Periodic boundary conditions are imposed in streamwise (x_1) and spanwise (x_2) directions.

When the momentum and energy equations are compared with each other, it is natural to notice that the main difference between the two equations is the existence of the Prandtl number term in the energy equation (Kim and Moin 1989). Na and Hanratty (2000) performed DNS of a turbulent channel flow with passive scalars at different molecular Prandtl numbers. The calculations were carried out, under isothermal wall boundary conditions, for passive scalar. The temperature (heat transfer) or mass concentration (mass transfer) were used as passive scalar.

Likewise, for example, temperature, thermal diffusivity, heat flux, and Prandtl number can be replaced with, respectively, concentration, diffusivity, mass flux and Schmidt number.

One of the ingredients in understanding turbulent transport of a scalar, between a flowing fluid and a flat solid surface, is the behavior of the fluctuating temperature and velocity fields close to the wall. The usual approach is to consider the system as fully developed velocity and temperature fields that exist in the boundary layer when the heated wall is held at constant dimensionless temperature. A DNS of the fully developed thermal field in a two-dimensional turbulent channel flow of air was carried out by Kasagi et al. (1992). The equations were derived for the isoflux boundary condition on the wall, so that the local mean temperature increased linearly in the streamwise direction. However, after the equations were transformed into dimensionless form, the isothermal boundary condition was used for the reference temperature equation, and the temperature fluctuations were assumed to be zero on the wall. The DNS assumption that the wall temperature fluctuations are zero, cannot explain the existence of the thermal pattern on the heated solid wall, placed into the turbulent flow. Such a pattern, often referred to as thermal streaks, was observed and studied in experiments carried out by Iritani et al. (1983) and Hetsroni et al. (1997).

In the numerical code a pseudo-spectral method is employed to solve the governing equations. In the homogeneous directions (x_1 and x_2), all the quantities are expressed by Fourier expansions. In the x_3-direction which is nonhomogeneous, the quantities are represented by Chebyshev polynomials. A full description of the numerical scheme can be found in PhD thesis of Lam (1989). In the present numerical study the bulk Reynolds number is 2600. The calculations were carried out in a computational domain of $L_1^+ \times L_2^+ \times L_3^+ = 1074 \times 537 \times 171$ wall units in the x_1, x_2 and x_3 directions with a resolution of 128 x 128 x 65. A non-uniform distribution of collocation points is used in the x_3 - direction due to the nature of the Chebyshev polynomials, and the first collocation point away from the wall is at $x_3^+ = 0.1$.

It is assumed that all fluid properties are constant and the buoyancy is neglected. As the initial condition a uniform distributed temperature field was projected on the velocity field. The heat transfer simulation was started after the velocity field had reached a steady state. Then once the velocity field was calculated at each time step, the temperature field was obtained by integrating the energy equation with the same grid system used for the velocity field. Two different thermal boundary conditions were considered assuming isothermal wall ($T_w = const.$) and constant heat flux ($q_w = const.$). The last assumption corresponds to our experimental case.

The effect of wall boundary condition on scalar transfer in a fully developed turbulent flume was studied by Tiselj at al. (2001) for Prandtl numbers Pr=1 and Pr= 5.4. Two types of thermal wall boundary conditions for the dimensionless temperature equation were studied: isothermal wall boundary conditions, and isoflux wall boundary conditions (BC). The profile of the mean temperature was not affected by the type of BC. However, the type of BC has a profound affect on the statistics of the temperature fluctuations in the near-wall region $x_3^+<10$. Comparison of near-wall statistics of temperature fluctuations shows that at Pr =1 the buffer part of the turbulent boundary layer significantly influence the scalar transfer in the conductive sublayer, whereas at Pr=5.4 the near-wall temperature field may be associated with predominant motion in the viscous sublayer.

Tiselj at al. (2001) gave in their paper detailed discussion on the code reliability. The numerical results show good agreement with the DNS simulations by Kawamura et al. (1998). Hence, we use numerical fields generated with this code to the present analysis. For this purpose sequences of about 50 instantaneous velocity and temperature fields taken at a regular time interval ($\Delta t^+ = 2.416$) were stored after solution for the temperature field reached the statistical steady state.

The streamwise component of convection velocity of thermal perturbation is determined by streamwise space-time correlation, i.e., $\Delta x_2 = \Delta x_3 = 0$. There are several ways to determine convection velocity. Here we are considering the signal convection velocity of temperature perturbations, following Kim and Hussain (1993), who investigated the signal convection velocity of velocity, pressure and vorticity perturbations. The signal velocity is the velocity with which the main portion of signal amplitude travels and it can be measured by the location of the peak of space-time cross-correlation in an instantaneous field. The convection velocities of temperature fluctuations along the channel are shown in Fig. 3 for two thermal boundary conditions: constant heat flux and for the isothermal wall. For comparison, the mean flow velocity and the streamwise component of convection velocity of velocity perturbation (V_{U1}^+) is plotted.

It is worth noting that for most of the outer part of the channel, say $x_3^+ > 20$, the convection velocities for the velocity perturbations are almost identical with the local mean flow velocity *U*. Near the wall, however, all convection velocities for perturbations exceed *U*, becoming constant for $x_3^+ < 10$. Also it can be seen that close to the wall ($x_3^+ < 10$) the convection velocities for

temperature and velocity perturbations are different, and that the velocity of temperature perturbations depends on the thermal boundary conditions imposed on the wall. In Fig. 3 we may see that at the bottom wall ($x_3^+ = 0$) the convective velocity of V_T^+ for the constant wall heat flux boundary condition is only 4.33 and for the isothermal wall it is 5.33, well below the convection velocity of velocity perturbations, which is approximately 10 in the wall region. For comparison Fig. 4 shows propagation velocity of the thermal perturbations for low Prandtl number flow (Pr=0.71). In this case the propagation velocities are significantly higher.

Our experimental visualization indicates the existence of thermal structures, which propagate streamwise, and are evident as appearing or disappearing of hot and cold spots. Their existence is related to the local bursts transporting fluid from or to the wall. These are known to travel for considerable streamwise distances without losing their identity (Hetsroni et al. 1997, 1999) and should therefore provide reliable information about the convection velocities. Hence, to identify them it should be more efficient to derive convection velocities from detection of typical thermal signatures. In order to address this problem, the convection velocity of strong temperature discontinuities on the bottom wall was studied. For this purpose an adaptation of the WAG (Window Average Gradient) algorithm was used (see Bisset et al. 1991). The WAG algorithm was developed to search for large-scale events by focusing on rapid transitions in the signal. The modified detection function is defined as

$$Sign[T(t_0 + \Delta t) - T(t_0)] \geq k\, T_{rms} \qquad (1)$$

where T represents the temperature, and k is the threshold parameter. The thermal fields, were evaluated at a time interval Δt^+=19.328, which was found to be the best time interval to determine the convection velocity by space-time correlation method. This time interval is also in agreement with the window length ($\Delta t^+ = 20$) used by Krogstad et al. (1998). If *Sign* is taken to be +1, detection triggers on rapid transition from low to high values of temperature. Perhaps this is characteristic of the transition from the end of a sweep to the beginning of an ejection. Conversely, for *Sign* = -1, the detection points may represent the end of an ejection and the onset of a sweep.

For the threshold parameter k set to 0 the whole thermal field is divided into two parts with increasing and decreasing temperature. The convection velocities of these two parts are shown in

Fig. 5 across the channel depth. It can be seen that the convection velocities for decreasing temperature (*Sign* = -1) are always faster than those for increasing temperature (*Sign* = +1) in the whole depth, and this effect is much pronounced in the near-wall region. The convection velocity of the temperature fluctuations obtained from the space-time correlations V_T falls the limits between V_{T+1} and V_{T-1}.

Similar picture is obtained for the flow under the constant wall temperature thermal condition, i.e. the convection velocities for temperature decreasing are always faster than those for temperature increasing. This shows that there is a general trend for the negative thermal discontinuities to be convected at a somewhat higher velocities than the positive ones. We have assumed that the negative thermal discontinuities are mainly linked to flow event of "end of an ejection and onset a sweep", and positive thermal discontinuities with "end of a sweep and the beginning of an ejection". This corroborates with the observations by Krogstad and Antonia (1994) of the streamwise pattern near large-scale positive discontinuities, and agrees with the results of Krogstad et al. (1998), where the convection velocity of velocity discontinuities were measured.

In Fig. 5 we may see that at the near-wall region the convective velocity V_T^+ obtained for the constant heat flux boundary conditions is 5.60 for the negative ("cold") transition, and only 3.24 for positive ("hot") transition. It is worth noting that these values are qualitatively in a good agreement with our experimental findings reported above for the convective velocity of the hot and cold thermal structures (dark and bright spots). However, there is still an open question if the displacements evaluated in the physical experiment from the thermal images are good representatives of the convective velocity of the thermal coherent structures visualized on the other side of the wall. To elucidate this problem, a sequence of synthetic images simulating thermal pattern at the wall was generated from the DNS solution. These images were analyzed in a same way as the physical images from the infrared sensor.

5. Image analysis of synthetic thermal images

The essential streak formation mechanism of near wall coherent flow structure is due to the localized lift-up of low-speed fluid near the wall by advecting streamwise vortices. Our image analysis of the thermal streaks indicates that their propagation velocity is close to that obtained in the numerical simulations for the convection velocity of the thermal structures. However, in our

method of analysis, an arbitrary selection of the threshold for hot/cold spots as well as the PIV based image processing procedure may introduce an unknown bias to the results obtained. Hence, we address the question now, if the behavior of the observed thermal "fingerprints" describes the underlying flow characteristics well enough. For this purpose the temperature field calculated on the wall is used to generate gray level contours simulating the IR images. Figure 6 shows isotherms calculated for the wall displayed as 64 - gray levels expanded to full 8 bit intensity range (0- 255). These synthetic images of the wall temperature show longitudinal structures similar to these observed in the experiment (Hetsroni et al. 2001). By applying the above-described PIV evaluation procedure to these images the convective velocity of the simulated thermal spots is found.

To compare this evaluation with our experimental data a sequence of 31 images simulating infrared maps was generated for water flow using the DNS simulation described above. Three different time intervals between images were used: $\Delta t^+ = 2.416$, 4.832 and 9.644. It was found that the most appropriate time interval for PIV analysis of the synthetic images was 4.832, close to that found for the experimental data.

For each sequence of images time and space average of the longitudinal convective velocity of "thermal" streaks was calculated, separately for "hot" and "cold" regions. Figure 7 shows histograms for the streamwise velocity obtained in such a way for a sequence of the synthetic images. We may note several similarities to Figure 1, showing the experimental data. The evaluated convective velocity is characterized by a rather broad distribution, especially for the "hot" spots. It may be due to a rather low resolution of the synthetic images, degrading our PIV analysis. Nevertheless, we may clearly distinguish difference in the mean velocity of the "cold" and "hot" spots. The mean values of convective velocity V_T^+ calculated for the whole sequence was found to be 4.44 for the cold spots, and 3.78 for the hot spots. Table 1 collects results of our two evaluations of convective velocities obtained from the experimental (PIV-EXP) and synthetic images (PIV-DNS). It is interesting to note that convective velocities obtained from the synthetic images are very close to our experimental averages, i.e. 4.77 and 3.76, respectively. Despite over three-fold difference in the Reynolds number, our physical and synthetic thermal streaks exhibit very similar behavior. This confirms that our "optical" evaluation method works correctly for both the experimental and the synthetic images. For both cases we also have qualitative agreement with the convective velocity of the "thermal signatures", (DNS row in Table 1). However, quantitatively they differ by more than 10% from the directly calculated convective

velocities of the thermal discontinuities, particularly for velocities of the "cold" spots. It is obvious that our PIV method of analysis can not exactly reproduce these values, as the analyzed thermal streaks are already the objects, which represent spatial temperature averages. Nevertheless their correlation with the "thermal signatures" defined for the DNS data is evident.

Some differences of the statistical characteristics of the evaluated convective velocities, already visible in the histograms, are described by standard deviation, skewness and flatness in Table 1. Generally, the experimental data show broader scatter, which is rather obvious. The evaluated distribution of convective velocity for both experimental and synthetic images, as well as DNS data, shows rather weak asymmetry (skewness about ±0.2). It may confirm that temperature fluctuations for high Prandtl number are greatly damped by molecular diffusion in wall region, as described by Na and Hanratty (2000). This affects convective velocities of the thermal perturbations and is responsible for observed dissimilarities between momentum and heat transport in a turbulent boundary layer (Kong et al. 2001).

6. Discussion

The main difficulty of heat transfer analysis in the near-wall region lies in the interaction between the molecular and turbulent heat transfer. Kim and Moin (1989) presented results pertaining to the transport of passive scalars in turbulent flow and thermal wall boundary condition T_w = const. The scalar fields are highly correlated with the streamwise velocity; the correlation coefficient between the temperature and the streamwise velocity is as high as 0.95. It is clear from Fig 4 that in this case convection velocity of temperature fluctuation is very close to that of velocity fluctuation. The Prandtl number and thermal wall boundary condition affect the interconnection between the thermal and kinematic characteristics of the turbulent fluctuations.

Examination of high-order statistical correlations, such as skewness, indicates a strong influence of thermal wall boundary condition on the temperature fluctuations in the wall region. This influence in the behavior of the temperature fluctuations can be observed also in the two-point spanwise correlations of temperature fluctuations. The spanwise separation of thermal streaky structures was identified with the negative peaks in the spanwise correlation, Tiselj et al. (2001). For both, isothermal and isoflux thermal wall boundary conditions, these peaks shift to smaller values of x_3^+ with increasing the Prandtl number. This is not surprising since the sublayer of the thermal boundary layer is a strong function of the Prandtl number. At Pr=1, temperature

and streamwise velocity fluctuations which obey the same boundary condition at the wall, diffuse in a similar manner. Thus they are transported similarly by the normal velocity fluctuations in the wall region and exhibit the same large-scale structures. It is well known that under isothermal wall boundary condition the statistics of temperature and streamwise velocity fluctuations are very similar. In contrast, at high Prandtl (Schmidt) number the temperature (or concentration) field is unable to diffuse efficiently in the wall region and follows directly the inflows and outflows associated with the bursting events. A striking feature of this situation is small- scale fluctuation in scalar fields, such as temperature, advected by turbulent flow. Dissimilarity between velocity and temperature fluctuations at Pr>1 leads to observed dissimilarity in their convection velocity.

Conclusions

The present analysis confirmed the ability of the PIV - based evaluation method to track the coherent thermal structures visualized at the wall by an IR camera. Our preliminary study shows that the temporal and spatial analysis of long time sequences of thermal images can be used to evaluate basic characteristics of the underlying fluid flow. It is shown that the mean convective velocity of coherent structures can be relatively well evaluated from the thermal pattern dynamics. It is worth noting that the method offers a unique opportunity to obtain basic flow characteristics without any optical or mechanical access to the flow. It may have great practical importance for studying turbulent transport in industrial installations.

Our analysis of the thermal structures confirms the DNS findings that under constant wall heat flux there is a general trend for the negative thermal discontinuities to be convected at somewhat higher velocities than the positive ones. Since the negative thermal discontinuities are mainly linked with the “end of an ejection and onset a sweep”, and positive thermal discontinuities with the “end of a sweep to the beginning of an ejection”, so it can be concluded that a high-speed fluid region followed by a low-speed region is convected at a higher speed than a low-speed fluid region followed by a region of higher velocity. It is qualitatively in agreement with observation done by Krogstad et al. (1998), who found up to 20% difference of the convection velocity between sweeps and ejections for a wind tunnel flow.

Under the conditions of our experiment, the time and space averaged dimensionless value of propagation velocity of coherent thermal structures obtained for hot spots was $V_T^+ = 3.76$ and for the cold spots was $V_T^+ = 4.77$. Very closed values were obtained using the same method of

analysis for the synthetic images generated from a direct numerical simulation of a similar flow. Our analysis of the DNS solution shows that the "thermal discontinuities" propagate at the velocity very close to that found from the image analysis of the thermal spots. Hence, we suppose that there is a strong correlation between the dynamics of the thermal structures observed on the wall and the momentum and heat transport in the turbulent boundary layer.

The DNS simulations allowed us to relate the propagation velocity of large-scale temperature structures to that of velocity perturbations. We confirmed dissimilarity between streamwise velocity and temperature fields in the near-wall region. It appears that this relation is highly dependent on the molecular Prandtl number. For fluids characterized by higher Prandtl number, like water used in the experiment, the convective velocity of coherent thermal structures is only about half of that for momentum transport. This is in general agreement with findings of Na and Hanratty (2000), who obtained for Pr=10 the convection velocity in near-wall temperature field $V_T^+ \approx 3.9$. For low Prandtl number fluid the difference is smaller and the convection velocity of thermal perturbation is about 90% of that for the velocity perturbations. This topic is certainly important and the momentum and heat transfer relations for the near-wall regions should be investigated in the future. Further studies seem necessary to obtain the proper relation of transport and mixing properties of the scalars for arbitrary Prandtl or Schmidt numbers.

Acknowledgments

This research was supported by the Center for Absorption in Science of the Ministry of Immigrant Absorption (State of Israel). This research was also supported by the Fund for the Promotion of Research at the Technion. A. Mosyak was supported by the Committee for Planning and Budgeting of the Council for Higher Education under the framework of the KAMEA Program. The authors express their gratitude to Dr Chenfeng Li, for his help in extracting data from the DNS simulations.

References

1. Bisset DK; Antonia RA; Raupach MR (1991) Topology and transport properties of large-scale organized motion in a slightly heated rough wall boundary layer. Phys. Fluids A3: 2220-2228

2. Herman C; Kang E; Wetzel M (1998) Expanding the application of holographic interferometry to the quantitative visualization of oscillatory thermofluid process using temperature as tracer. Exp. Fluids 24: 431-436
3. Hetsroni G; Kowalewski TA; Hu B; Mosyak A (2001) Tracking of coherent thermal structures on a heated wall by means of IR thermography. Exp. Fluids 30**:** 286-294
4. Hetsroni G; Mosyak A; Rozenblit R; Yarin LP (1999) Thermal patterns on the smooth and rough walls in turbulent flows. Int. J. of Heat Mass Transfer 42: 3815-3829
5. Hetsroni G; Mosyak A; Yarin LP (1997) Thermal streaks regeneration in the wake of a disturbance in a turbulent boundary layer. Int. J. of Heat Mass Transfer 40: 4161-4168
6. Hetsroni G; Rozenblit R (1994) Heat transfer to a liquid solid mixture in a flume. Int. J. Multiphase Flow 20: 671-689
7. Hetsroni G; Rozenblit R; Yarin LP (1996) A hot-foil infrared technique for studying the temperature field of a wall. Measurement Science and Technology **7**: 1418-1427
8. Hetsroni G; Zakin JL; Mosyak A (1997) Low-speed Streaks in Drag-Reduced Turbulent Flow. Phys. Fluids 9: 2397-2404
9. Iritani Y; Kasagi N; Hirata N (1983) Heat transfer mechanism and associated turbulence structure in the near wall region of a turbulent boundary layer. In Fourth Symposium on Turbulent Shear Flows. Karlsruhe, Germany, 12-14 September, pp. 17.31-17.36
10. Kaftori D; Hetsroni G; Banerjee S (1994) Funnel-shaped vortical structures in wall turbulence. Phys. Fluids 6: 3035-3050.
11. Kasagi N; Tomita T; Kuroda A (1992) Direct Numerical Simulation of Passive Scalar Field in a Turbulent Channel Flow. J. Heat Trans. 114: 598-606.
12. Kawamura H; Abe H; Matsuo Y (1999) DNS of Turbulent Heat Transfer in Channel Flow with respect to Reynolds and Prandtl Number effects. Int. J. Heat and Fluid Flow 20: 196-207
13. Kawamura H; Ohsaka K; Abe H; Yamamoto K (1998) DNS of Turbulent Heat Transfer in Channel Flow with Low to Medium-High Prandtl Number Fluid. Int. J. Heat and Fluid Flow 19: 482-491
14. Kim J; Hussain F (1983) Propagation velocity of perturbations in turbulent channel flow. Phys. Fluids 5: 695-706
15. Kim J; Moin P (1989) Transport of Passive Scalars in a Turbulent Channel Flow. In: Turbulent Shear Flows, vol 6. Springer, Heidelberg Berlin New York, 85-96

16. Kong H; Coi H; Lee JS (2001) Dissimilarity between the velocity and temperature fields in a perturbed turbulent thermal layer. Phys. Fluids 13: 1466-1479
17. Krogstad PA; Antonia RA (1994) Structure of turbulent boundary layers on smooth and rough walls. J. Fluid Mech. **277**: 1-21.
18. Krogstad PA; Kaspersen JH; Rimestad S (1998) Convection velocities in a turbulent boundary layers. Phys. Fluids 10 : 949.
19. Lam KK (1989) Numerical Investigation of Turbulent Flow Bounded by a Wall and a Free-Slip Surface. Ph.D. Thesis. Univ. California, Santa Barbara.
20. Moin P; Mahesh K (1998) Direct Numerical Simulation: A Tool in Turbulence Research. Annu. Rev. Fluid Mech. 30: 539-578
21. Na Y; Hanaratty TJ (2000) Limiting behavior of turbulent transport close to a wall. Int. J. Heat Mass Trans. 43**:** 1749 -1758
22. Qu not GM; Pakleza JM; Kowalewski TA (1998) Particle image velocimetry with optical flow. Exp. Fluids 25: 177-189.
23. Taylor GI (1921) Diffusion by continuous movements. Proc. Lond. Math. Soc. 20: 196-212.
24. Tiselj I; Pogrebnyak E; Li C;Mosyak A; Hetsroni G (2001) Effect of wall boundary condition on scalar transfer in a fully developed turbulent flume. Phys. Fluids 13: 1028-1039
25. Warhaft Z (2000) Passive scalars in turbulent flows. Annu. Rev. Fluid Mech. 32: 203-240

List Figures and Tables

Table 1. Evaluation of the mean convective velocity of thermal perturbations, standard deviation (Std), skewness (S) and flatness (F); image processing based velocity obtained for the experimental IR images (PIV-EXP) and for the synthetic images from DNS data (PIV-DNS). DNS – values of convective velocity of velocity (V_U) and temperature (V_T) perturbations evaluated from the numerical fields.

	V_U	V_T Sign=-1 (cold spots)				V_T Sign=+1 (hot spots)			
	mean	mean	Std	S	F	mean	Std	S	F
PIV-EXP	n.a.	4.77	2.34	0.11	2.94	3.76	2.33	-0.17	3.15
PIV-DNS	n.a.	4.44	1.35	0.21	2.92	3.78	1.35	0.25	2.91
DNS	10	5.60	n.a.	0.14	2.75	3.24	n.a.	0.14	2.75

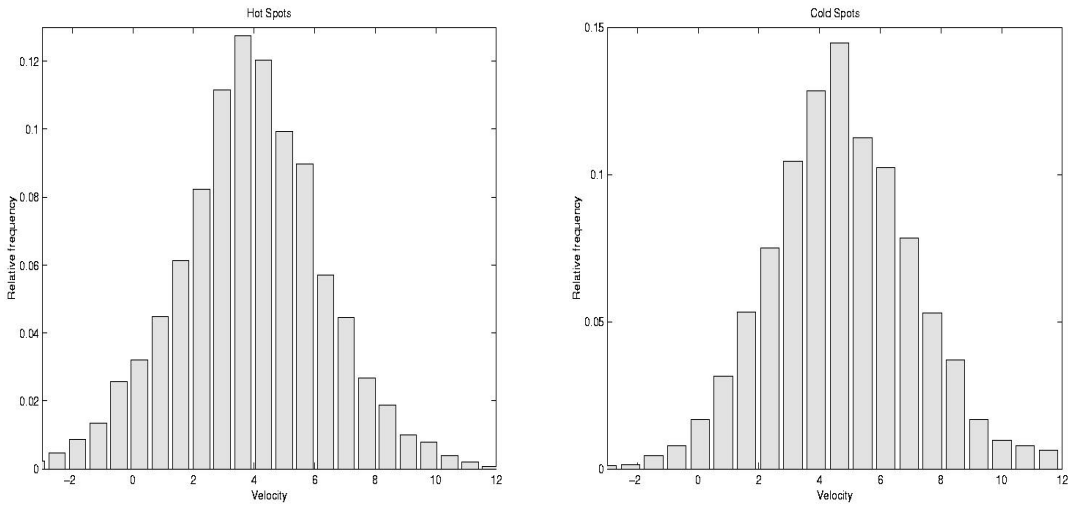

Figure 1. Histograms of non-dimensional streamwise velocity evaluated for a sequence of the IR images; left – hot spots evaluation, mean velocity $V_T^+ = 3.76$, right – cold spots evaluation, mean velocity $V_T^+ = 4.77$.

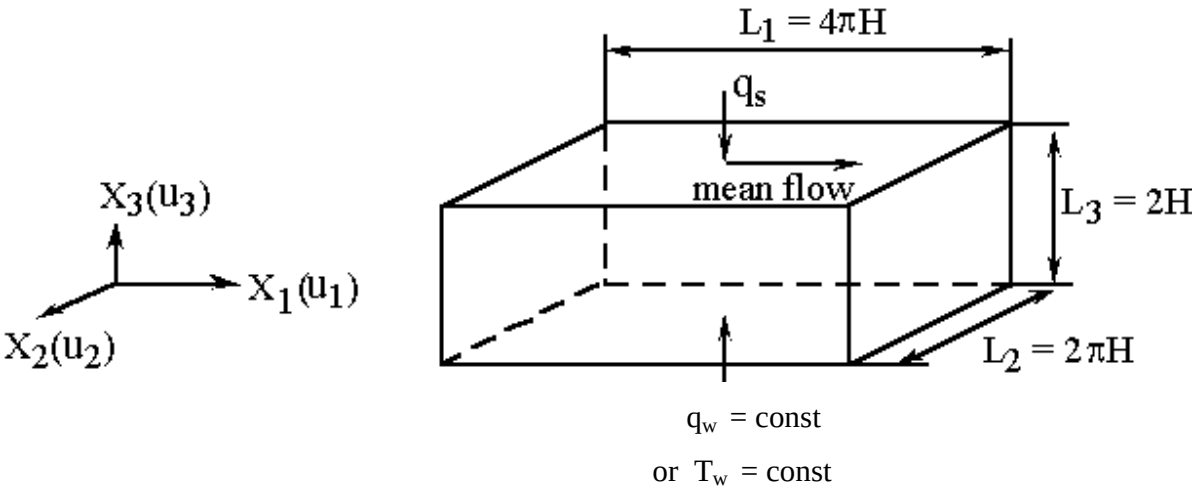

Figure 2. Computational domain, coordinate system and thermal wall boundary conditions

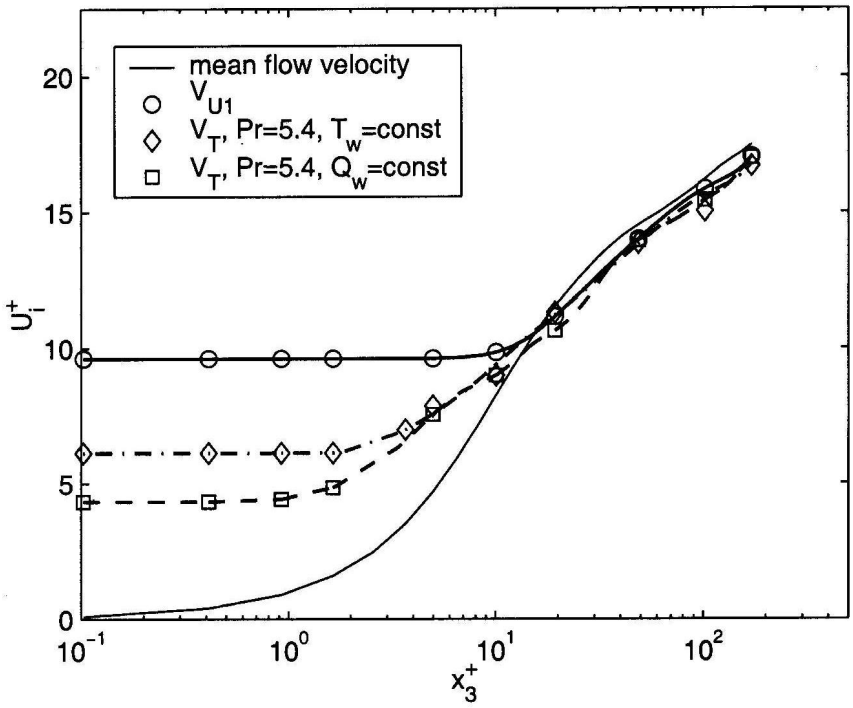

Figure 3. Convection velocities of thermal discontinuities V_T across the channel depth calculated for water flow (Pr=5.4) under the isothermal wall and constant wall heat flux boundary condition; compared with the mean flow velocity profile (solid line) and convection velocity of velocity perturbations V_{U1}.

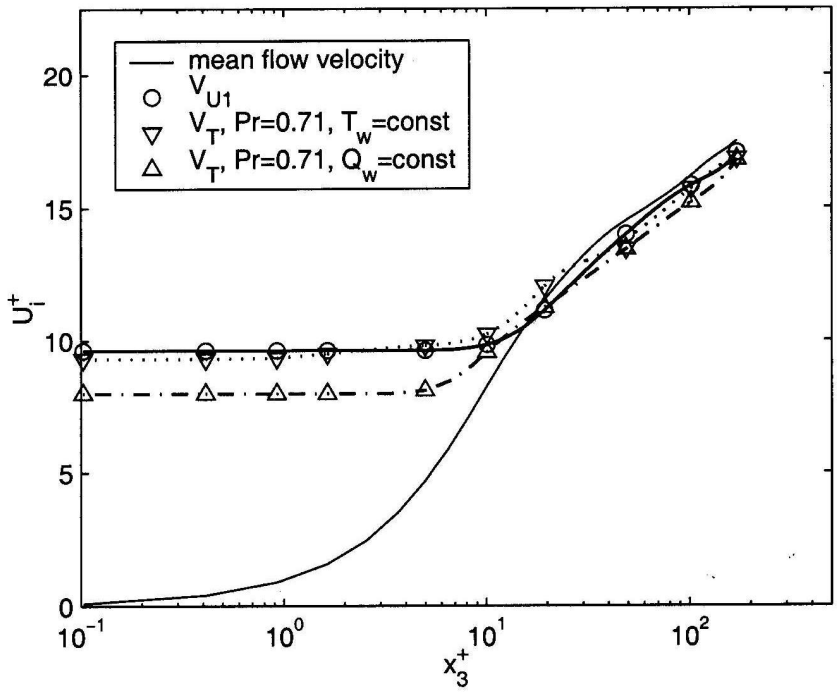

Figure 4. Convection velocities of temperature perturbations across the channel depth for low Prandtl number flow (Pr=0.7).

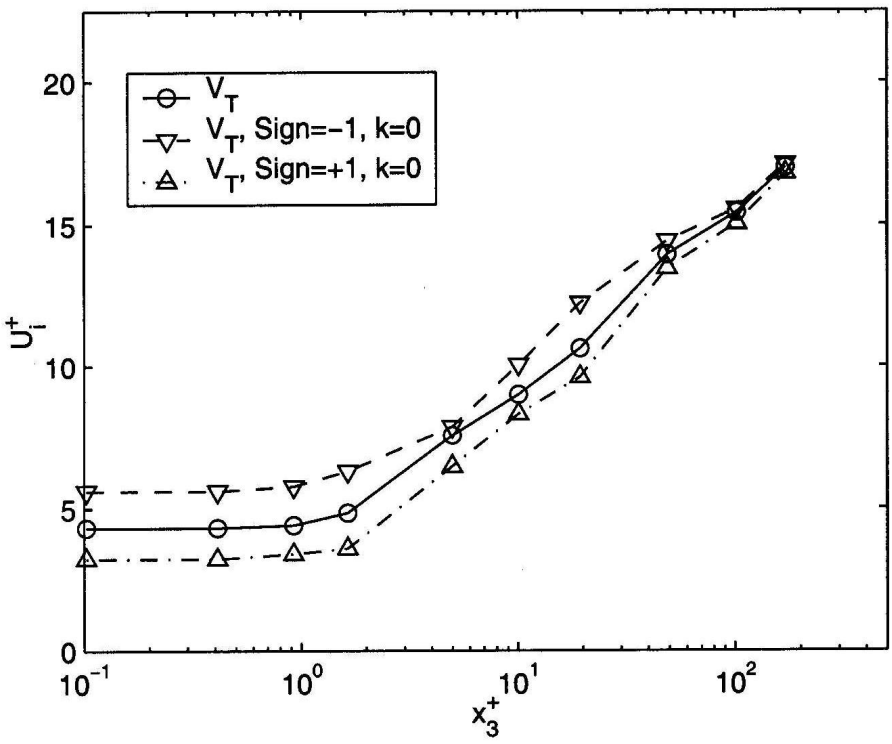

Figure 5. Convection velocity of temperature perturbations V_T across the channel calculated for water flow for constant heat flux boundary conditions; mean velocity and velocity of "cold" (Sign=-1) and "hot" (Sign=+1) sweeps.

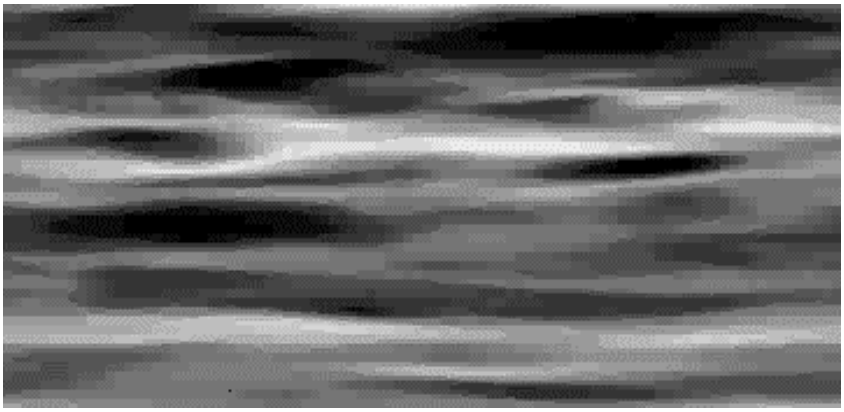

Figure 6. Synthetic image of the wall temperature field generated from the DNS solution.

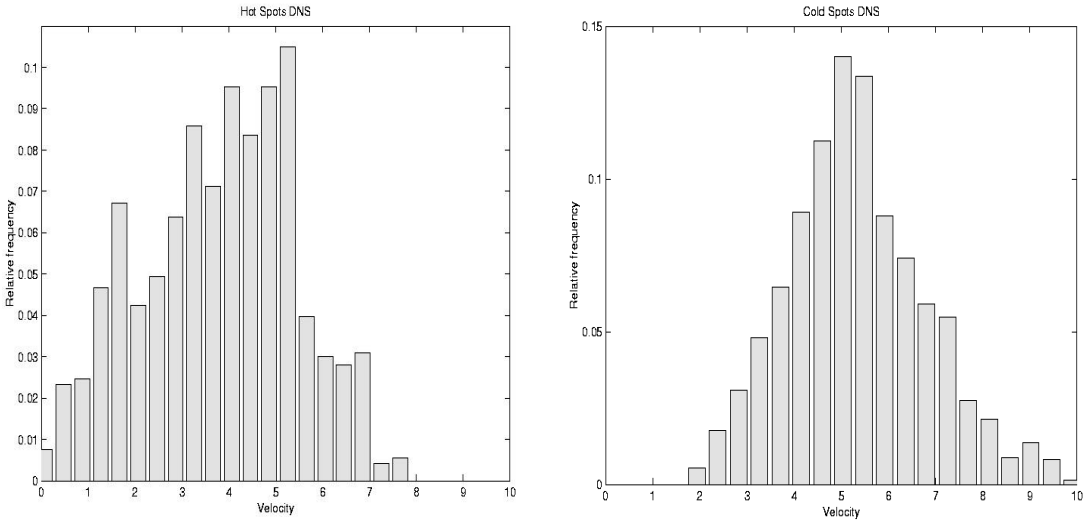

Figure 7. Histograms of non-dimensional streamwise velocity of the wall thermal structures evaluated for a sequence of 10 images generated from the DNS solution; $\Delta t^+ = 4.832$; left – hot spots evaluation, mean velocity $V_T^+ = 3.78$, right – cold spots evaluation, mean velocity $V_T^+ = 4.44$.